PKR-MEDIATED STRESS RESPONSE ENHANCES DENGUE AND ZIKA VIRUS REPLICATION

Taissa Ricciardi-Jorge[1*], Edroaldo Lummertz da Rocha[1], Edgar Gonzalez-Kozlova[1,2], Gabriela Flavia Rodrigues-Luiz[1], Brian J Ferguson[2], Nerea Irigoyen[2], Daniel Santos Mansur[1*]

[1] Departamento de Microbiologia, Imunologia e Parasitologia, Centro de Ciências Biológicas (CCB), Universidade Federal de Santa Catarina (UFSC), Florianópolis, SC, Brasil.

[2] Present address, Icahn School of Medicine, New York, USA.

[3] Department of Pathology, University of Cambridge, Tennis Court Road, Cambridge, UK.

* corresponding authors: daniel.mansur@ufsc.br; taissarj@gmail.com

ABSTRACT

The mechanisms by which *Flaviviruses* use non-canonical translation to support their replication in host cells are largely unknown. Here we investigated how the integrated stress response (ISR), which promotes translational arrest by eIF2α phosphorylation (p–eIF2α), regulates *Flavivirus* replication. During Dengue virus (DENV) and Zika virus (ZIKV) infection, eIF2α activation peaked at 24 hours post infection and was dependent on PKR but not type I interferon. The ISR is activated downstream of p-eIF2α during infection with either virus, but translation arrest only occurred following DENV infection. Despite this difference, both DENV and ZIKV replication was impaired in cells lacking PKR, independent of IFN-I/NF-kB signaling or cell viability. By using a ZIKV 5'UTR reporter system as a model, we found that this region of the genome is sufficient to promote an enhancement of viral mRNA translation in the presence of an active ISR. Together we provide evidence that *Flaviviruses* escape ISR translational arrest and co-opt this response to increase viral replication.

36 **INTRODUCTION**

37 The Flavivirus genus is part of the *Flaviviridae* family and contains the causative
38 agents of several human diseases of high global impact, such as: DENV, ZIKV, Japanese
39 encephalitis virus (JEV), yellow fever virus (YFV), West Nile virus (WNV) and others.
40 Flaviviruses are enveloped ssRNA(+)viruses of about 50 nm in diameter with 10-11 kb
41 genome containing a single ORF flanked by two non-coding segments (UTRs) 5´- (capped)
42 and 3'- (non-polyadenylated) (Chambers *et al*, 1990). Flavivirus replication is cytoplasmic in
43 strong association with ER, forming viral replication complexes by convolution of ER
44 membrane (Gillespie *et al*, 2010).

45 Despite the presence of a 5´-cap on its genome, DENV has been shown to use a
46 cap-independent mechanism for protein synthesis under the suppression of cap-binding
47 protein, eIF4E (Edgil *et al*, 2006). Using DENV and ZIKV, this mechanism was later shown to
48 be mediated by an internal ribosomal entry site (IRES localized in viral -UTR (Song *et al*,
49 2019). A recent report has confirmed the existence of the IRES element (Fernández-García
50 *et al*, 2020), indicating, along with previous suggestions (Hou *et al*, 2017; Edgil *et al*, 2006;
51 Roth *et al*, 2017) that a cap-dependent translation would be used for viral polyprotein synthesis
52 until the suppression of canonical translation initiation when a switch to cap-independent
53 translation would take place. This alternative cap-independent mechanism, including cell
54 conditions to promote the switch in translation mode, remains to be fully characterized.

55 A well-known cellular control over the translation machinery is coordinated by four
56 kinases of the integrated stress response (ISR), that act as sensors of different stressors.
57 They are: (i) PKR, activated by dsRNA; (ii) HRI, activated by oxidative stress and/or heme
58 deficiency; (iii) PERK, activated by reticulum stress; and GCN2, (iv) activated by deprivation
59 of amino acids (Donnelly *et al*, 2013; Pakos-Zebrucka *et al*, 2016; Wek *et al*, 2006). Therefore,
60 ISR is capable of detecting viral infections directly by dsRNA or indirectly via structural or
61 metabolic stresses. A shared target of these four kinases is the subunit alpha of the translation
62 factor eIF2 (eIF2α), which is part of the ternary complex (TC, eIF2-GTP-$tRNA_i^{Met}$), necessary
63 for translation initiation. Phosphorylation of eIF2α (p-eIF2α) prevents the exchange of the
64 associated inactive GDT for the active GTP, blocking its recycling for participation in the
65 formation of new 43S complexes, thus inhibiting general cell translation (Krishnamoorthy *et*
66 *al*, 2001; Jackson *et al*, 2010).

67 In the present work, we investigated how ISR impacts Flavivirus replication. We show
68 that PKR is the main kinase leading to eIF2α phosphorylation and cellular protein translation
69 arrest during infection. This event, however, is linked to the establishment of an optimal cellular
70 environment for virus replication. Using ZIKV as a model, we suggest that the ability to use
71 ISR pathway activation to enhance replication is restricted to the 5´-UTR. We hence
72 demonstrate that eIF2α phosphorylation is required for optimal viral replication.

RESULTS

DENV4 and ZIKV can induce ISR activation during infection

Interferon stimulated genes are central for Flavivirus restriction, therefore we used human lung A549 cells, as they support DENV and ZIKV replication and also produce and respond to type one interferons (IFN-I) (Wang *et al*, 2018; Whelan *et al*, 2019; Gullberg *et al*, 2018; Zhang *et al*, 2018; Song *et al*, 2019; Espada *et al*, 2019). We evaluated eIF2α phosphorylation during DENV4 and ZIKV infection as a marker of ISR activation by these viruses. By immunoblot analysis, we show that both viruses induce p–eIF2α by 24 hours post infection (h.p.i.) (Figure 1A). This time point coincides with PKR activation by autophosphorylation (Thr451), which suggests the participation of this kinase in ISR activation. Quantification by flow cytometry enables us to determine that eIF2α phosphorylation happens after 12 h p.i. reaching a peak at 24 h p.i. (Figure 1B). This time frame is surprisingly late, considering that from at least 12 h p.i. infectious virus particles can already be detected in cell supernatant under these experimental conditions (data not shown).

To further investigate the context of eIF2α phosphorylation, cells were co-stained with a monoclonal antibody directed against the flavivirus envelope protein (Figure 1C-D). At 24 h p.i. DENV4 infected cells exhibited a significant double-positive population, with about 90% of p–eIF2α+ cells being infected. However, during ZIKV infection, there is a lower proportion of double-positive cells, with about 40% of envelope positive cells in the p–eIF2α+ population. These cells may be infected with ZIKV, but they do not yet express enough envelope protein to allow detectable staining. The same profile of co-staining quantified by cytometry could also be visualized by immunofluorescence (Figure 1D).

In summary, although both infections led to different profiles of anti–p–eIF2α and anti–flavivirus co-staining, both viruses promote stress responses within the same time frame.

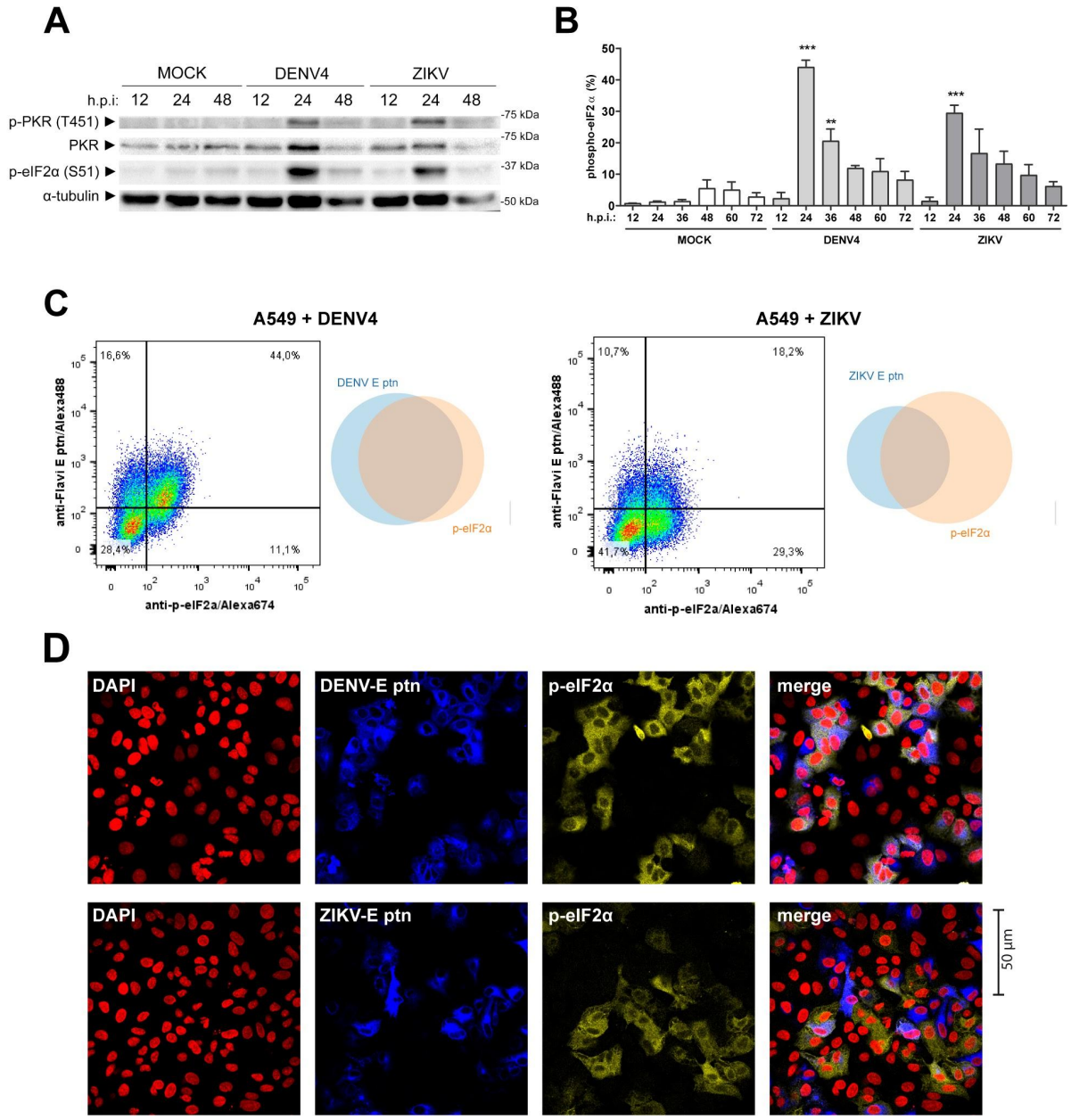

Figure 1 – DENV4 and ZIKV promote phosphorylation of eIF2α in A549 cells. A549 cells were infected with DENV4 (MOI 2) or ZIKV (MOI 3) and harvested at the indicated times for analysis. (A) Immunoblot analysis of cell extracts resolved in denaturing SDS-PAGE. (B) Flow cytometry analysis for quantification of cells expressing p–eIF2α within the total population (C) Dot plot and Venn diagram of representative results from co-staining with anti-Flavivirus E protein and anti-p–eIF2α at 24 h p.i. analysed by flow cytometry and (D) immunofluorescence of infections under the same conditions. In the column chart, the bars represent the means ± SEM. Statistical analysis was performed by paired *t* test comparing infected samples to the respective uninfected control. *: p ≤0.05; **: p ≤0.01; ***: p ≤0.001; ns / no markup: no statistical difference; h.p.i: hours post-infection.

Phosphorylation of eIF2α during DENV4/ZIKV infection is PKR-dependent and IFN-I independent

To investigate which ISR kinase promotes eIF2α phosphorylation in our model, gene deletion by CRISPR-Cas9 was used to produce A549 PKR and IFNAR knockout cell lines. In PKR$^{-/-}$ cells infected with DENV4 or ZIKV p–eIF2α was abrogated indicating that ISR activation promoted by both viruses is mostly dependent on this kinase (Figure 2A,B). Since PKR is an IFN-stimulated gene (ISG), and considering the late ISR activation, the participation of IFN-I signalling in eIF2α phosphorylation was assessed. However, there was no change in the level of p–eIF2α in infected IFNAR$^{-/-}$ A549s compared to WT cells (Figure 2A,B). This result also suggests that constitutive expression levels of PKR are sufficient for ISR activation. Likewise, experiments using a PKR/IFNAR double-knockout lineage confirmed the requirement for constitutive PKR expression to drive eIF2α phosphorylation.

The persistence of a small population p–eIF2α+ in the PKR$^{-/-}$ cells infected with ZIKV, indicates the activation of other ISR kinase by this virus. To investigate PERK activity, a selective inhibitor, GSK2656157 (Axten *et al*, 2013), was used. GSK2656157 treatment did not alter the induction of p–eIF2α in DENV4 infected cells but promoted a small decrease in p–eIF2α population in ZIKV infected cells (Figure 2C). This demonstrates a minor participation of PERK in the ISR activation in the ZIKV model.

In summary, the phosphorylation of eIF2α during infection by DENV4 or ZIKV is mainly PKR dependent and IFN-I independent in this model.

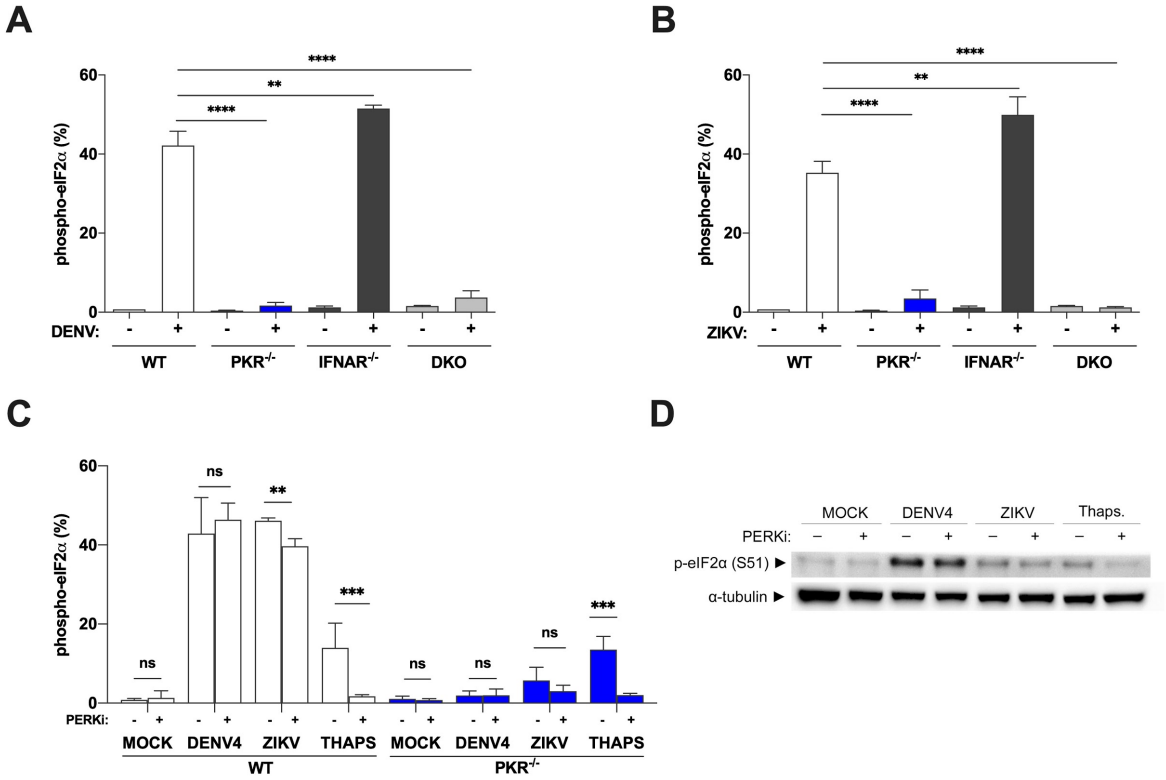

130 **Figure 2 – Phosphorylation of eIF2α during DENV4 or ZIKV infections is PKR-dependent**
131 **and IFN-independent**. (A) Flow cytometry analysis for quantification of cells expressing p–
132 eIF2α within the total population of the indicated lineages of A549 cells infected with DENV4
133 (MOI 2) at 24 h p.i.; and (B) same experiment using ZIKV (MOI 3) (C) Flow cytometry analysis
134 for quantification of cells expressing p–eIF2α within the total population A549 WT and $PKR^{-/-}$
135 cells infected with DENV4 (MOI 2) or ZIKV (MOI 3) or treated with thapsigargin 2μM for 45
136 minutes in the presence or absence of the PERK inhibitor GSK2656157 (5 μM) for 24h; and
137 (D) immunoblot analysis of cell extracts from the same experiment resolved in denaturing
138 SDS-PAGE. DKO: double $IFNAR^{-/-}/PKR^{-/-}$ knockout. In column charts, the bars represent the
139 mean ± SEM. Statistical analysis was performed by one-way ANOVA, followed by Tukey's
140 test for multiple comparisons.*: $p \leq 0.05$; **: $p \leq 0.01$; ***: $p \leq 0.001$; ns / no markup: no statistical
141 difference.
142
143 **PKR is not blocked by DENV4 or ZIKV but shows delayed recognition dsRNA**
144 The late PKR activation during infection with both viruses is not explained by the need
145 of type I IFN signaling to boost PKR levels. Therefore, we tested whether PKR activity is
146 blocked by infection at earlier time points. To test this, the dsRNA analogue, poly (I:C), was
147 used to stimulate PKR. Poly (I:C) transfection was performed at 3 h p.i. and cells were
148 analyzed at 9 h p.i., that is, before virus-promoted eIF2α phosphorylation (Figure 3A). The
149 comparable levels of p–eIF2α between mock and infected cells stimulated with poly(I:C)
150 suggest that PKR is not blocked by DENV4 or ZIKV in the early stages of infection (Figure
151 3B). The absence of p–eIF2α in $PKR^{-/-}$ cells demonstrates that eIF2α phosphorylation induced
152 by poly (I:C) is also dependent on this kinase.
153 If PKR is not blocked in the early stages of infection by DENV or ZIKV, the late ISR
154 activation could be due to the inability of RNA sensors such as PKR to access viral dsRNA,
155 as suggested previously (Fredericksen & Gale, 2006; Espada-Murao & Morita, 2011; Overby
156 *et al*, 2010). To test this hypothesis, infected cells were incubated in a semisolid medium so
157 viral spread happens from cell to cell by juxtaposition allowing temporal inferences of events
158 based on cell location from the centre of the viral plaque. Immunofluorescence of DENV4
159 infected cells shows that cells at the edge of the viral plaque do not phosphorylate eIF2α
160 despite the presence of dsRNA (Figure 3C). This result indicates that ISR activation is
161 delayed, occurring in infected cells after the establishment of viral replication complexes.
162

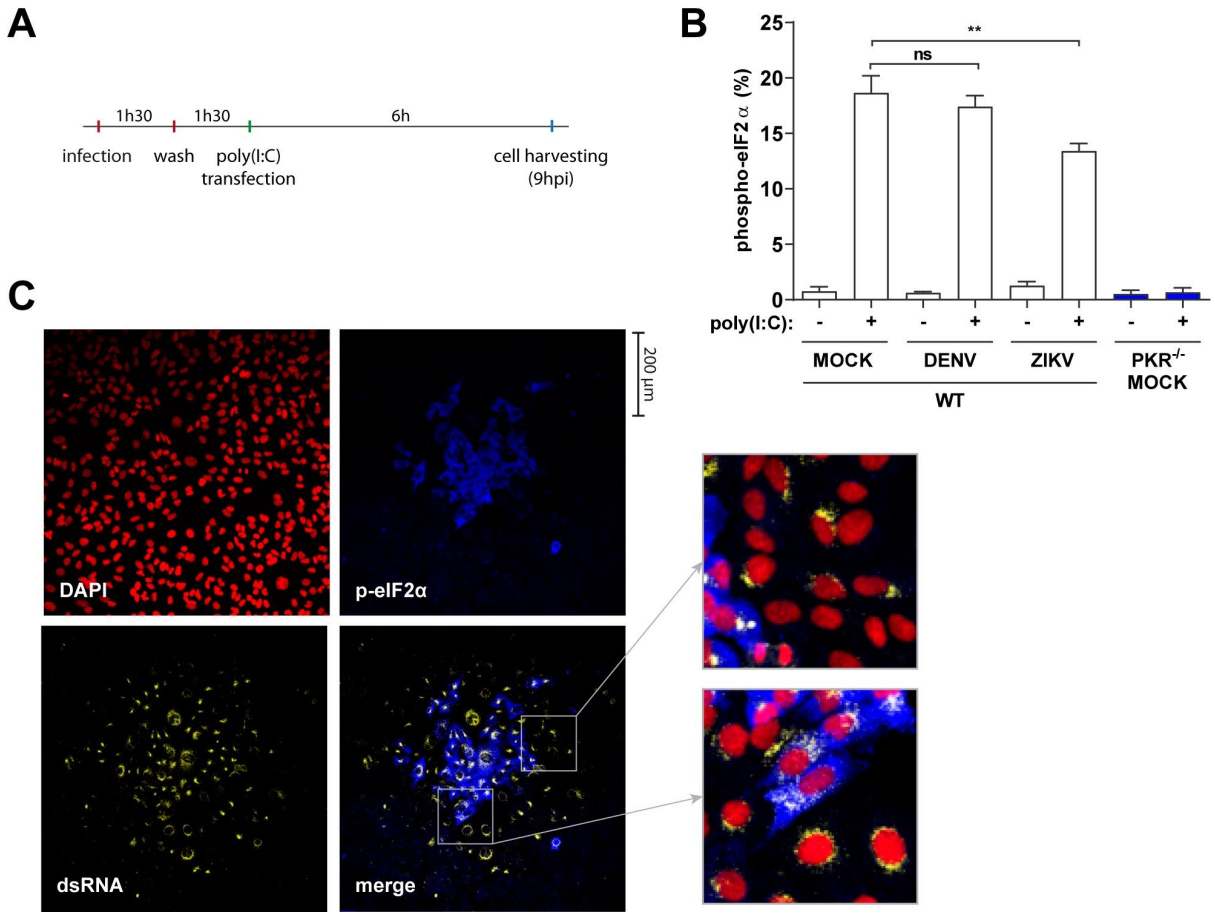

Figure 3 – PKR is not blocked by DENV4 or ZIKV but shows delayed recognition dsRNA. (A) Schematic representation of the assay design. Cells were infected with MOCK/DENV4/ZIKV and incubated for 1h30 before wash, then stimulated with poly(I:C) at 10 µg/ml for 6 hours. (B) Flow cytometry analysis for quantification of cell population expressing p–eIF2α after stimulation with poly (I:C). Data obtained from two independent experiments. (C) Immunofluorescence of A549 WT cells infected with DENV4 for 48 h p.i. in semisolid medium. Cells fixed, permeabilized and co-stained with DAPI, anti-dsRNA and anti-p–eIF2α. In the column chart, the bars represent the means ± SEM from three independent experiments. Statistical analysis was performed by one-way ANOVA, followed by Tukey's test for multiple comparisons. *: p ≤0.05; **: p ≤0.01; ***: p ≤0.001; ns / no markup: no statistical difference.

DENV4, but not ZIKV, induces translation arrest in infected cells

To investigate the consequences of eIF2α phosphorylation on cellular and viral protein translation, viral infections were performed in semi-solid medium and a puromycin labelling protocol was used to assess general translation activity (Schmidt *et al*, 2009). By immunofluorescence analysis, it was possible to observe that p–eIF2α in WT lineage promotes cellular translation arrest during DENV4 infection, evidenced by the absence of

182 puromycin incorporation in the centre of viral plaques (Figure 4A). At the edges of the plaque,
183 however, anti-puromycin and anti-flavivirus simultaneous staining reinforces data presented
184 previously (Fig 3C) that translation arrest happens relatively late during DENV4 infection. In
185 $PKR^{-/-}$ cells, however, co-staining is present throughout the viral plaque, suggesting cell
186 translation downregulation during DENV4 infection is caused by ISR activation via PKR.
187 Surprisingly for ZIKV, there is a different profile, with more intense incorporation of
188 puromycin by infected WT cells than bystander cells (Figure 4B). Bystander cells are here
189 defined as cells that were in the same environment of infected cells (i.e. same well or
190 organism) but a viral protein or nucleic acid was not detected. Anti-puromycin signal is
191 stronger in the perinuclear region which coincides with viral replication sites (Figure 4C). The
192 phenotype of increased translation activity in infected cells is lost in $PKR^{-/-}$ cell lines,
193 suggesting that PKR activation allows increased viral translation.

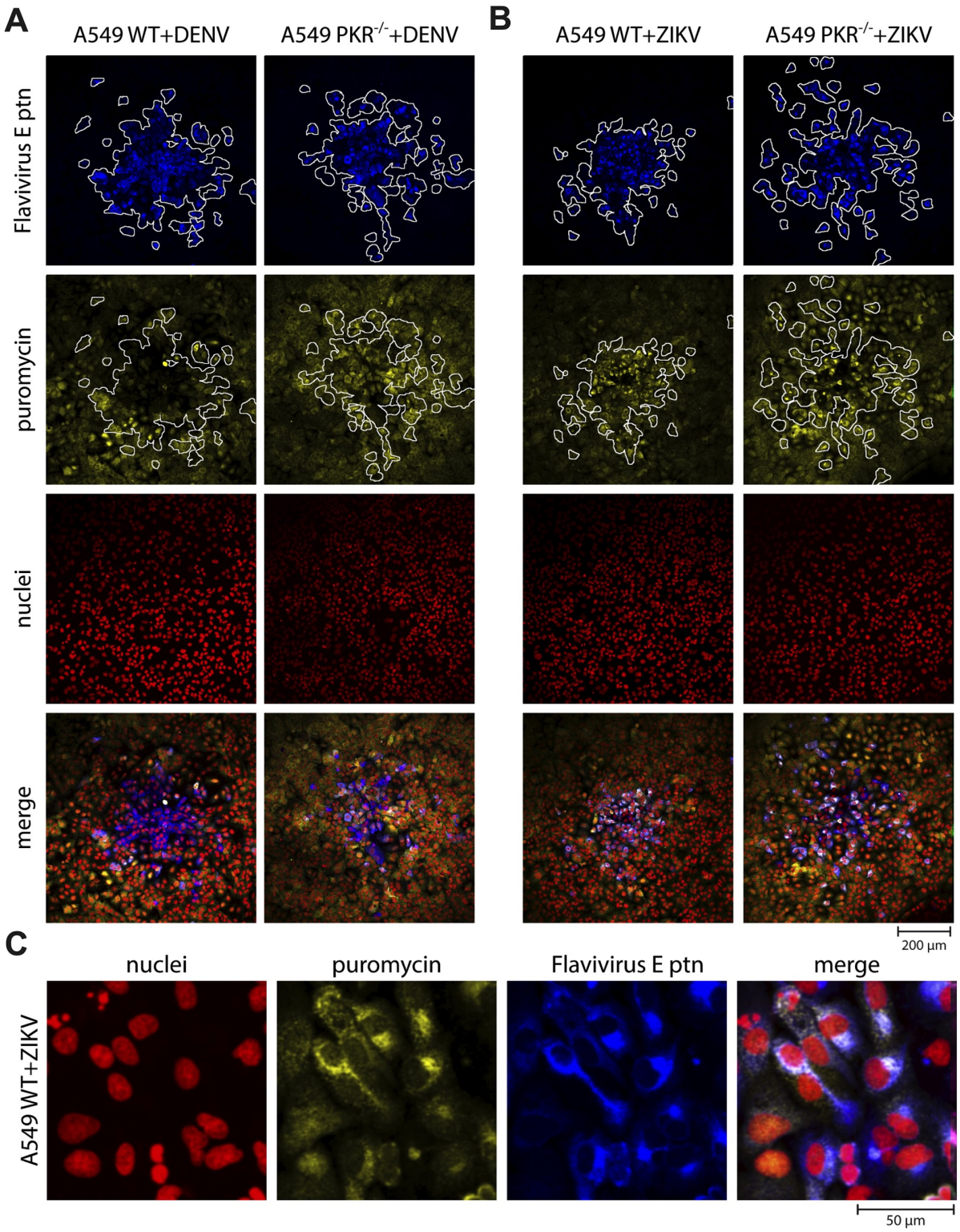

Figure 4 - DENV4, but not ZIKV, induces PKR-dependent translation arrest in infected cells. Immunofluorescence of A549 WT or PKR$^{-/-}$ cells infected with DENV4 (A) or ZIKV (B) for 48 h p.i. in semisolid medium. Cells labelled with puromycin before fixation and permeabilization. Co-staining with DAPI, anti-puromycin, anti-flavivirus envelope (E) and secondary antibodies. (C) Zoom on WT cells infected with ZIKV for a better appreciation of the immunostaining pattern. Representative images of three different experiments.

PKR is required for expression of eIF2α-downstream genes and proteins during DENV4/ZIKV infections

Phosphorylation of eIF2α also leads to transcriptional up-regulation of genes from cellular stress resolution pathways (Harding *et al*, 2000; Novoa *et al*, 2001). To evaluate the impact of PKR deficiency in events downstream of eIF2α phosphorylation, the expression of *DDIT3* (CHOP) and *GADD34* was analysed. Gene transcription was evaluated by qPCR (Figure 5A) and both *DDIT3* and *GADD34* were less expressed in PKR$^{-/-}$ cells during DENV4/ZIKV infection than in WT cells. This downregulation is subtle probably due to control of these genes by other pathways such as IRF3/7 (Clavarino *et al*, 2012; Dalet *et al*, 2017) and STAT3-NFkB or NF-YA (Huang *et al*, 2010; Canino *et al*, 2015). However, when GADD34 expression is analyzed by immunoblot (Figure 5B) or flow cytometry (Figure 5C) the downregulation of this protein follows p–eIF2α profile. These results are in line with the literature since GADD34 mRNA translation requires p–eIF2α to suppress uORF2 reading, which in turn inhibits the CDS translation (Lee *et al*, 2009; Young *et al*, 2015), demonstrating the transcriptional and post-transcriptional cellular control over eIF2α downstream signalling.

In summary, these results show that during infection by DENV4/ZIKV the activation of the stress response is not restricted to phosphorylation of PKR and eIF2α; and reinforces that the activation of this pathway is abolished in the PKR$^{-/-}$ cells.

Figure 5 – PKR is required for expression of eIF2α-downstream genes and proteins during DENV4/ZIKV infections. A549 WT or PKR-/- cells infected with DENV4 (MOI 2) or ZIKV (MOI 3) and harvested at 24 h p.i. for analysis. (A) Quantification by RT-qPCR of DDIT3 and GADD34 gene expression. Relative expression calculated by 2-ΔΔCt methods using mock WT cells as reference. (B) Immunoblot analysis of GADD34 protein expression. (C) Flow cytometry analysis for quantification of cells expressing GADD34 within the total population. In the column chart, the bars represent the means ± SEM from three independent experiments. Statistical analysis was performed by paired *t* test comparing the two cell lineages under the same conditions. *: p ≤0.05; **: p ≤0.01; ***: p ≤0.001; ns / no markup: no statistical difference.

231 **Disruption of the PKR–eIF2α pathway impairs DENV4 and ZIKV replication**

232 Considering the efficacy of p-eIF2α in blocking cellular translation and the
233 dependency of PKR for this phosphorylation, we evaluated the impact of PKR deletion on virus
234 replication. Surprisingly, replication of both viruses was impaired in PKR$^{-/-}$ cells, shown by
235 lower virus titres (Figure 6A) and smaller plaque sizes and number of cells/plaque (Figure 6B-
236 C), but no difference in genome replication as assessed by qPCR (Figure 6D).

237 The lower virus titres and diminished plaque sizes in PKR$^{-/-}$ cells are particularly
238 counterintuitive since this cell line is defective in activating the whole antiviral pathway
239 coordinated by PKR. This finding indicated the possibility that the PKR deletion has a negative
240 impact on other antiviral pathways and/or these viruses could have co-opted the ISR to
241 promote viral replication.

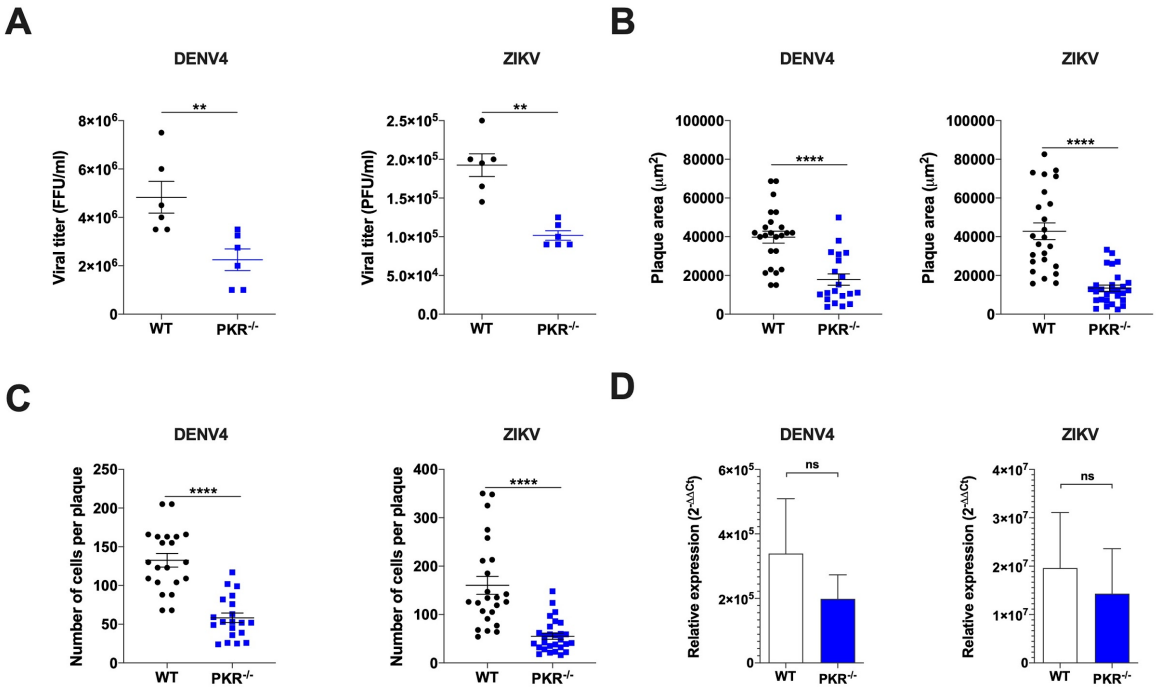

242

243 **Figure 6 - Disruption of the PKR–eIF2α pathway impairs DENV4 and ZIKV replication.**
244 (A) Viral titration from A549 WT or PKR$^{-/-}$ cells infected with DENV4 (MOI 2) or ZIKV (MOI 3)
245 and harvested at 24 h p.i. for analysis. . Plaque size comparison of virus in A549 WT or PKR-
246 /- cells infected with DENV4 and incubated for 8 days or infected with ZIKV and incubated for
247 5 days: measurements of (B) plaque areas and (C) number of cells per plaque from
248 immunofluorescence. (D) Quantification by RT-qPCR of DENV4 or ZIKV viral RNA from A549
249 WT or PKR$^{-/-}$ cells infected with DENV4 (MOI 2) or ZIKV (MOI 3) and harvested at 24 h p.i.
250 for analysis. Relative expression calculated by $2^{-\Delta\Delta Ct}$ method using mock WT cells as a
251 reference. PFU: plate forming units; FFU: focus forming units. In the column chart, the bars
252 represent the means ± SEM from three independent experiments. Statistical analysis was

253 performed by paired *t* test comparing the two cell lineages under the same conditions. *: p
254 ≤0.05; **: p ≤0.01; ***: p ≤0.001; ns / no markup: no statistical difference.
255
256 **PKR deletion does not affect the innate immune response or cell viability**
257 The phenotype of reduced viral replication in PKR$^{-/-}$ lineage could be explained by
258 changes in the cellular innate immune response, as several studies report the role of PKR in
259 sustaining NF-kB and IFN signalling (Gilfoy & Mason, 2007; Zamanian-Daryoush *et al*, 2000;
260 Czerkies *et al*, 2018; Deb *et al*, 2001; Kårehed *et al*, 2007) and promoting IFNγ and TNFα
261 expression (Kaempfer *et al*, 2019; Ben-Asouli *et al*, 2002). To investigate the possibility of
262 alterations in innate immune pathways as a result of PKR deletion, gene and protein
263 expression of elements of this response was evaluated.
264 Genes activated by IRF3/7, IFN-I or NF-κB did not show any significant difference in
265 transcription between WT and PKR$^{-/-}$ lineages during virus infections (Figure 7A).
266 Immunoblotting corroborated this transcriptional analysis, as no differences were observed in
267 STAT1 activation or IFIT1 and ISG15 expression levels between the two cell lines, thus
268 demonstrating virus-induced IFN-I signalling is not affected by PKR deletion (Figure 7B).
269 As PKR can also play a role in cell survival during viral infections (Donzé *et al*, 2004),
270 cell viability was analyzed at 24 h p.i. by cytometry. Also in this assay, no difference between
271 WT and PKR$^{-/-}$ lineages was observed during virus infections (Figure 7C).
272 Together, this set of results allow us to conclude that the PKR deletion does not
273 significantly affect the innate immune response or cell survival during DENV4 or ZIKV
274 infection. Therefore, alterations in these pathways do not explain the lower viral replication
275 seen in the PKR$^{-/-}$ cells.

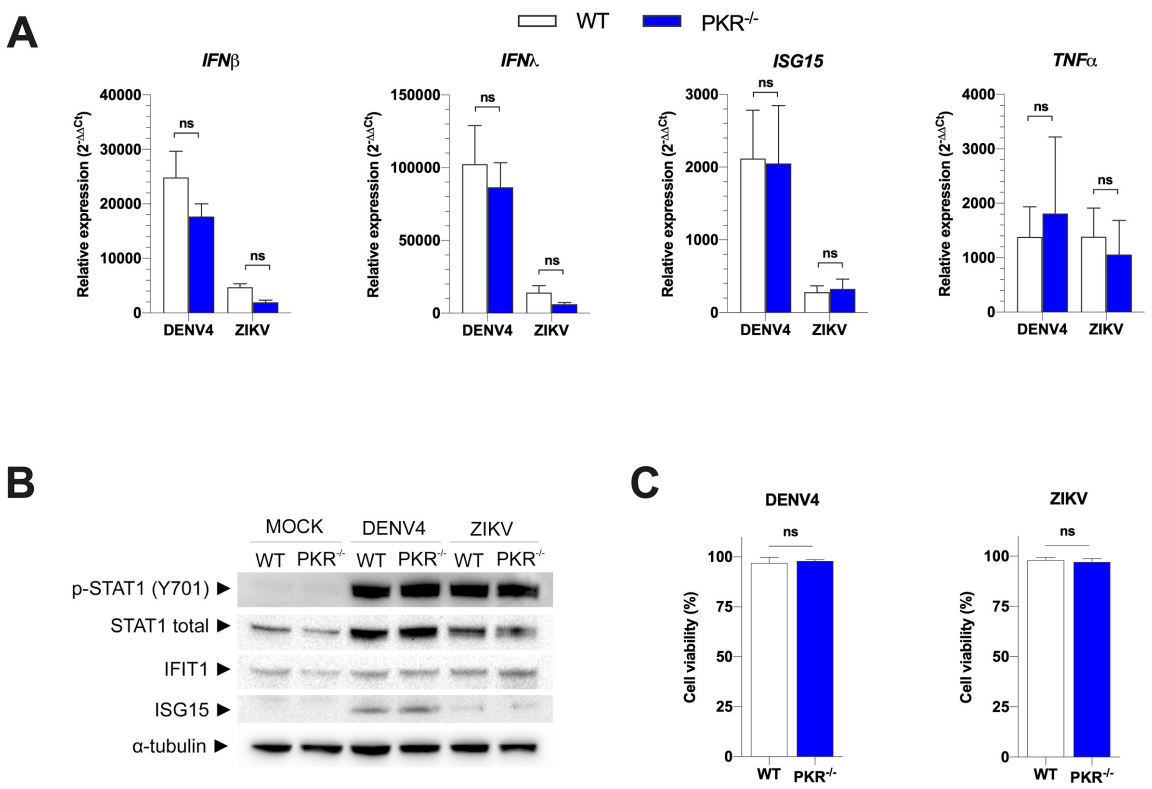

Figure 7 - PKR deletion does not affect the innate immune response or cell viability. A549 WT or PKR-/- cells infected with DENV4 (MOI 2) or ZIKV (MOI 3) and harvested at 24 h p.i. for analysis. (A) Quantification by RT-qPCR of IFNB, IFNL, ISG15 and TNFA1 gene expression. Relative expression calculated by 2-ΔΔCt methods using mock WT cells as a reference. (B) Immunoblot analysis of cell extracts resolved in denaturing SDS-PAGE. (C) Flow cytometry analysis for quantification of living cells by staining with Zombie-NIR viability dye. Mock WT cells set as 100% reference. In the column chart, the bars represent the means ± SEM from three independent experiments. Statistical analysis was performed by paired *t* test comparing the two cell lineages under the same conditions. *: p ≤0.05; **: p ≤0.01; ***: p ≤0.001; ns / no markup: no statistical difference.

ZIKV coopts PKR–eIF2α pathway to increase viral translation through its 5´-UTR

ISR control over cell translation can promote the expression of certain mRNAs as a consequence of their 5´-UTR sequence and/or structure (Young *et al*, 2015; Young & Wek, 2016). Therefore, we next sought to investigate whether viral 5´-UTR could subvert the ISR to promote replication. Hence, a translation activity assay was performed based on the ZIKV genome using a luciferase reporter readout. For this assay, a reporter plasmid was designed with the first 194 nucleotides of ZIKV, this includes the 5´-UTR followed by the first 87 nt from the viral polyprotein fused in frame with the firefly luciferase gene (Figure 8A). A control plasmid for expression of *Renilla* luciferase with the same backbone that the firefly luciferase

297 reporter was co-transfected for data normalization. Results are presented in Relative
298 Translation Activity (RTA), given in percentage, using values obtained with WT mock cells as
299 reference (100%).
300 Cells were infected with ZIKV for 12 hours before plasmid transfection, then analysed
301 at 36 h p.i. to maximize the time of luciferase expression. The comparison between mock and
302 infected conditions for each cell line reveals that virus infection promotes a 2-fold increase in
303 translation activity by WT and IFNAR$^{-/-}$ cells (Figure 8B). In contrast, in PKR$^{-/-}$ and double
304 knockout cells this effect is suppressed as relative translation activity in these cells, under
305 infected and uninfected conditions, is similar or lower to WT uninfected cells. These results
306 suggest that the ZIKV 5´-UTR is sufficient to promote a relative advantage of mRNA translation
307 in the presence of p–eIF2α.

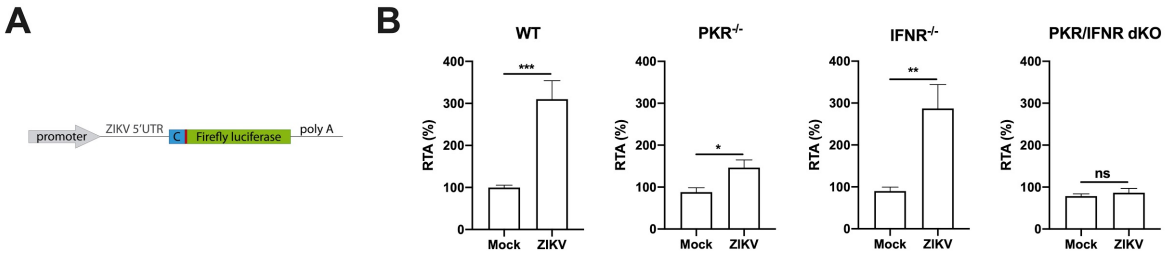

308
309 **Figure 8 - ZIKV 5´-UTR is sufficient to increase relative reporter translation in PKR–**
310 **eIF2α competent cells**. (A) Diagram of reporters constructs used for the assay. (B) Relative
311 translation of ZIKV reporter in A549 (WT/PKR$^{-/-}$/IFNAR$^{-/-}$/DKO) cells infected with ZIKV (MOI
312 3), transfected at 12 h p.i. and analysed at 36 h p.i. C: first 87 nt of viral capsid protein. In the
313 column chart, the bars represent the means ± SEM from three independent experiments. *: p
314 ≤0.05; **: p ≤0.01; ***: p ≤0.001; ns / no markup: no statistical difference.
315
316 **DISCUSSION**
317 Given the *Flavivirus* genome structure, its is suggested that these viruses would use
318 a cap-dependent translation mechanism for viral polyprotein synthesis until the suppression
319 of canonical initiation machinery when a switch to cap-independent translation would take
320 place (Edgil *et al*, 2006; Fernández-García *et al*, 2020). Cell conditions to promote the switch
321 in translation mode and the required auxiliary factors (eIFs) for alternative translation remain
322 to be fully characterized.
323 In the present work, we investigated how ISR, known to promote translation arrest
324 through eIF2α phosphorylation, would play a role in this elusive non-canonical translation
325 mechanism employed by flaviviruses. Using A549 cells we verified that basal levels of PKR
326 are sufficient to promote p-eIF2α during DENV4 and ZIKV infections. In accordance, previous
327 reports have also detected p-eIF2α in A549 cells during DENV (Umareddy *et al*, 2007), ZIKV
328 (HOU, S. et al., 2017; ZHOU et al., 2019) and JEV (TU et al., 2012) infections; as well as

329 studies using other cell lines (Peña & Harris, 2011; Tan *et al*, 2018). Further characterization
330 of p-eIF2α was performed by flow cytometry to allow quantification and co-staining for other
331 markers. Although DENV4 and ZIKV promote eIF2α phosphorylation within the same time
332 frame, these viruses displayed different profiles of anti–p–eIF2α and anti–flavivirus co-
333 staining, indicating distinct dynamics between viral replication and activation of stress
334 response for each virus. Therefore, cytometry is here proposed as a complementary method
335 to investigate ISR activation, in addition to traditionally used immunoblot and
336 immunofluorescence, as it can provide more detailed information.

337 It is worth noting that a few studies attribute to PERK/UPR the phosphorylation of
338 eIF2α observed during flavivirus infections without excluding the participation of other ISR
339 kinases in the phenotype (Gladwyn-Ng *et al*, 2018; Datan *et al*, 2016; Wang *et al*, 2019;
340 Sharma *et al*, 2017; Ambrose & Mackenzie, 2011). However, in the present model, PERK
341 plays a minor role in ZIKV-induced p-eIF2α. Here, PKR is clearly accountable for ISR
342 activation during infection with both DENV4 and ZIKV. This response was shown to be
343 activated from PKR to p-eIF2α-downstream genes in WT lineage but abolished in $PKR^{-/-}$
344 lineage.

345 An increased expression of p-eIF2α downstream genes was also found in Huh7 cells
346 infected with DENV (Zanini *et al*, 2018a). In this study, single-cell RNA-seq analysis showed
347 upregulation of *DDIT3* and *GADD34* (aka *PPP1R15A*) mRNAs, as well as of other ATF4-
348 downstream genes (*ASNS, CTH, HERPUD1, SOD2, TRIB3*) (Gjymishka *et al*, 2009; Dickhout
349 *et al*, 2012; Ma & Hendershot, 2004; Fusakio *et al*, 2016; Ohoka *et al*, 2005) within the infected
350 population (Supplementary Figure 1A-B). A second study using the same approach in PBMC
351 (Zanini *et al*, 2018b) revealed an upregulation of *GADD34* mRNA in DENV-infected monocytes
352 and T cells (Supplementary Figure 1C-D). The upregulation of these mRNAs suggests ISR
353 activation after DENV infection in these cell models. However, as shown here, the expression
354 of these genes are also regulated by post-transcriptional mechanisms dependent on the
355 presence of p-eIF2α.

356 In our model, a PKR-dependent translation arrest was confirmed in DENV-infected
357 cells as expected, but curiously not in ZIKV-infected cells. For the latter, increased puromycin
358 incorporation in perinuclear areas indicates a possible viral escaping mechanism from ISR
359 translation control. This difference might be related to the distinct dynamics between viral
360 replication and activation of stress response for each virus seen in the co-staining assay.
361 Therefore, it calls for further investigation using methods such as live-cell imaging, to track
362 down the sequence of events during infection.

363 Roth et al, reported a general translation arrest after infection of Huh7 cells with
364 several *Flavivirus* species and strains despite the absence of p-eIF2α (Roth *et al*, 2017). This
365 conflicting result could be due to the different cell lineage used. Although we do not exclude

366 the possibility that other translation suppression mechanisms, such as RIDD (HOLLIEN;
367 WEISSMAN, 2006), RNase L (DONOVAN et al., 2017) and 4E-BP dephosphorylation (Pause
368 *et al*, 1994; Poulin *et al*, 1998), can also take place in our model in later times after infection.
369 Despite the differences in translational activity under activated ISR, both DENV4 and
370 ZIKV presented an approximated 50% less viral replication in PKR$^{-/-}$ cells. This decrease
371 suggests that ISR activation is not essential for viral replication but rather co-opted by both
372 viruses to counter a major cellular antiviral pathway for their own benefit. Indeed, after
373 discarding the hypothesis of PKR deletion disturbing common antiviral pathways (e.g. type I
374 IFN expression, NFkB activation and apoptosis) translation activity assay has shown that ZIKV
375 5´-UTR promotes a relative advantage of mRNA translation in the presence of p–eIF2α. This
376 finding reveals that ZIKV not only escapes ISR translation arrest, but also uses this response
377 to increased viral replication. Moreover, it also indicates that viral alternative translation does
378 not require eIF2/TC for initiation. The independence of eIF2 for translation initiation under
379 stress conditions has been previously reported within *Flaviviridae* family, since HCV
380 (*Hepacivirus* genus) and *Pestivirus C* (formerly CSFV, *Pestivirus* genus) IRES present similar
381 functioning (Pestova *et al*, 2008; Robert *et al*, 2006; Rivas-Estilla *et al*, 2002).
382 Here we demonstrate that DENV and ZIKV induce eIF2α phosphorylation in a PKR
383 dependent manner and that its absence is detrimental for optimal virus replication. Using ZIKV
384 as a model we showed that this effect maps to the 5'UTR of the viral genome. Altogether
385 these results suggest that the activation of the PKR/p-eIF2α axis may be necessary for the
386 engagement of the non-canonical translation employed by Flaviviruses.
387

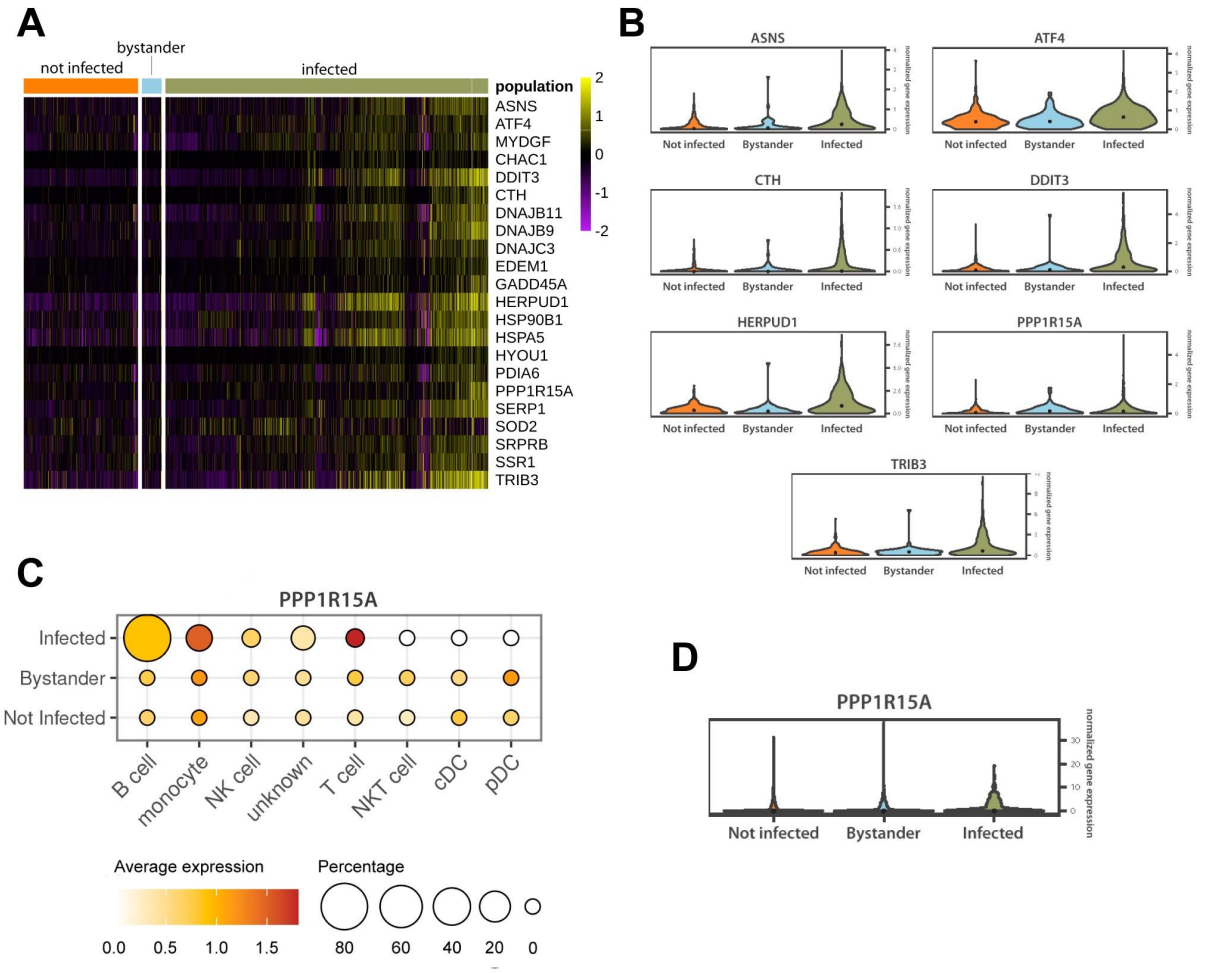

Supplementary figure 1 – p–eIF2α-downstream genes are upregulated in DENV-infected Huh7 cells and PBMCs. (A) Dataset from (Zanini *et al*, 2018a), of DENV-infected Huh7 cells, analysed by single-cell RNA-seq. Heatmap representing expression variability of stress-related genes in uninfected, bystander and infected cells; and (B) violin plot representing the expression of p-eIF2α- and ATF4-downstream genes in uninfected, bystander and infected cell populations. (C) Dataset from (Zanini *et al*, 2018b), of PBMCs from patients infected with DENV, analysed by single-cell RNA-seq. Dot plot representing the expression of PPP1R15A/GADD34 in different cell population and infection conditions; and (D) violin plot representing the expression of PPP1R15A/GADD34 the whole PBMC population under uninfected, bystander and infected conditions.

MATERIALS AND METHODS

Cells and viruses. VERO-E6 (ATCC® CRL-1586™) A549 (ATCC® CCL-185™) and derived cell lines were grown at 37° C/5% CO2 in DMEM-F12 medium supplemented with 1 U/ml penicillin /streptomycin and 5% fetal bovine serum. C6/36 cells (ATCC® CRL-1660 were grown at 28° C in Leibovitz's L-15 medium supplemented with 1 U/ml penicillin /streptomycin and 5% fetal bovine serum. IFNAR1 knockout cell line has been previously

406 described (Antunes *et al*, 2019; Guimarães *et al*, 2019). PKR$^{-/-}$ and DKO (IFNAR$^{-/-}$/PKR$^{-/-}$) were
407 produced with a pair of sgRNA guides (PKR1-FWD: CACCGATTATGAACAGTGTGCATCG;
408 PKR1-REV: AAACCGATGCACACTGTTCATAATC; PKR2-
409 FWD:CACCGAAACAGTTCTTCGTTGCTTA; PKR2-REV:
410 AAACTAAGCAACGAAGAACTGTTTC) cloned into pSpCas9(BB)-2A-Puro (PX459) vector
411 (Addgene) according to developer's protocol (Ran *et al*, 2013).
412 DENV-4 virus, TVP-360 strain (KUCZERA et al., 2016) and ZIKV, strain BR
413 2015/15261 (STROTTMANN et al., 2019) were kindly provided by Dr Claudia N. Duarte dos
414 Santos (Fiocruz-PR, Brazil). Viral stocks were produced in C6/36 cells and all viral titrations
415 were performed in VERO cells by plaque-forming units (PFU) or focus-forming units (FFU).
416 **Poly (I:C)Transfection**. Cell stimulation with poly (I:C) ("polyinosinic: polycytidylic
417 acid") was performed with Lipofectamine 3000 (Invitrogen) following manufacturer's
418 instructions for A459 cells at the proportion of 1 ug of poly(I:C) in 1 ml of medium in a 12-well
419 plate.
420 **Western-blots**. Samples were lysed on ice with RIPA buffer (150 mM NaCl; 50 mM
421 Tris-HCl pH8; 1% NP40; 0.1% SDS; 0.5% sodium deoxycholate) supplemented with
422 cOmplete™ and PhosSTOP inhibitors™ (Roche) according to manufacturer's
423 recommendations. Protein extracts were heat-denatured in loading buffer and resolved in
424 SDS-PAGE. Antibodies used for immunoblot reactions were: PKR antibody (Santa Cruz
425 Biotechnology, Inc, sc-707, dilution 1:100); phospho-PKR (Thr451) polyclonal antibody,
426 Invitrogen, 44-668G, dilution 1:100); phospho-eIF2α (Ser51) antibody (Cell Signaling
427 Technology, Inc., #9721, dilution 1:1000); GADD34 antibody (Proteintech, 10449-1-AP,
428 dilution 1:500); α-tubulin (DM1A) mAb (Cell Signaling Technology, Inc., #3873, dilution
429 1:1000); STAT1 antibody (AbCam, ab3987, dilution 1:1000); phospho-STAT1(Y701) M135
430 (Abcam, ab29045, dilution 1:1000); IFIT1 polyclonal antibody (Thermo/Pierce, PA3-848,
431 dilution 1:1000); ISG15 mouse mAb (R&D System, MAB4845, dilution 1:1000); anti-mouse
432 IgG, HRP-linked Antibody (Cell Signaling Technology, Inc., #7076, dilution 1:5000); anti-rabbit
433 IgG, HRP-linked Antibody, Cell Signaling Technology, Inc., #7074, dilution 1:5000). The
434 imaging of blots was carried out on the Chemidoc MP (Bio-Rad).
435 **Flow cytometry**. Cells were fixed in BD-Phosflow Lyse/Fix buffer. Primary and
436 secondary antibodies were diluted in permeabilization buffer (0.1% saponin; 1% fetal bovine
437 serum, in PBS) for staining. Between each step, samples were washed in blocking buffer (1%
438 fetal bovine serum in PBS). Antibodies and dyes used for flow cytometry were: phospho-eIF2α
439 (Ser51) antibody (Cell Signaling Technology, Inc., #3597, dilution 1:300); human monoclonal
440 antibody DV 18.4 (Beltramello *et al*, 2010)(dilution 1:100); GADD34 antibody (Proteintech,
441 10449-1-AP, dilution 1:250 (IF/FACS); Zombie-NIR fixable viability dye (BioLegend, 423105,
442 dilution 1:750); Goat anti-Rabbit IgG (H+L) Alexa Fluor 647 conjugated (Invitrogen, A-21245,

443 dilution 1:500); Goat anti-Rabbit IgG (H+L) Alexa Fluor 488 conjugated (Invitrogen, A-11008,
444 dilution 1:500); Goat anti-Human IgG (H+L) Alexa Fluor 488 conjugated (Invitrogen, A-11013,
445 dilution 1:500). Data acquisition was performed with FACSVerse™ (BD) and data analysis
446 with FlowJo software (BD).

447 **Immunofluorescence**: Cells were grown and infected on 13 mm cover slips in 24-
448 wells plates and incubated in liquid or semisolid medium according to experiment design.
449 Fixation in 3% paraformaldehyde for 20 minutes and permeabilization with Triton X-100 0,5%
450 in PBS for 5 minutes. Primary and secondary antibodies were diluted in blocking buffer (2%
451 bovine serum albumin in PBS) for staining. Between each step, samples were washed in PBS.
452 Antibodies and dyes used for immunofluorescence were: DAPI (Invitrogen); anti-dsRNA MAb
453 J2 (SCICONS, 10010500, dilution 1:200); human monoclonal antibody DV 18.4 (Beltramello
454 *et al*, 2010)(dilution 1:100); anti-puromycin 12D10 (Millipore, MABE343, dilution 1:20,000);
455 phospho-eIF2α (Ser51) antibody (Cell Signaling Technology, Inc., #3597, dilution 1:300); Goat
456 anti-Rabbit IgG (H+L) Alexa Fluor 647 conjugated (Invitrogen, A-21245, dilution 1:500); Goat
457 anti-Rabbit IgG (H+L) Alexa Fluor 488 conjugated (Invitrogen, A-11008, dilution 1:500); Goat
458 anti-Human IgG (H+L) Alexa Fluor 488 conjugated (Invitrogen, A-11013, dilution 1:500);
459 Donkey Anti-Mouse IgG H&L Alexa Fluor 647 conjugated (Abcam, ab150107, dilution 1:500).
460 Image acquisition was performed in the confocal microscope Leica DMI6000 B.

461 **RT-qPCR**:RNA was extracted and purified with HiYield TotalRNA mini kit (RBC Real
462 Biotech Corporation, YRB50) according to manufacturer's instructions. Reverse transcription
463 reaction was performed with MMLV "in house" kit from 1 µg of total RNA. Quantitative PCRs
464 were performed with GoTaq ® qPCR Master mix (Promega) with the following primer sets:
465 h18S (F: 5'-TAGAGGGACAAGTGGCGTTC-3', R: 5'-CGCTGAGCCAGTCAGTGT-3'); hIFNL1
466 (F: 5'-TTCCAAGCCCACCACAACTG-3', R: 5'-GAGTGACTCTTCCAAGGCGT-3'); hIFNB1 (F:
467 5'-AAACTCATGAGCAGTCTGCA-3', R: 5'-AGGAGATCTTCAGTTTCGGAGG-3'); hTNFA (F:
468 5'-TCTTCTCGAACCCCGAGTGA-3', R: 5'-CCTCTGATGGCACCACCAG-3'); hISG15 (F: 5'-
469 TCCTGGTGAGGAATAACAAGGG-3', R: 5'-TCAGCCAGAACAGGTCGTC-3'); hDDIT3 (F: 5'-
470 GGAGCATCAGTCCCCCACTT-3', R: 5'-TGTGGGATTGAGGGTCACATC-3'); hGADD34 (F:
471 5'-CTGGCTGGTGGAAGCAGTAA-3', R: 5'-TATGGGGGATTGCCAGAGGA-3'); DENV4
472 vRNA (F: 5'-TTGTCCTAATGATGCTGGTCG-3', R: 5'-TCCACCTGAGACTCCTTCCA-3');
473 ZIKV vRNA (F: 5'-CTGTGGCATGAACCCAATAG-3', R: 5'-ATCCCATAGAGCACCACTCC-
474 3'). Data acquisition with StepOne Plus real time PCR system (Applied Biosystems) and
475 relative mRNA expression was calculated by $2^{-\Delta\Delta CT}$ method.

476 **ZIKV Luciferase reporter vectors**: The pSGDLuc vector previously described
477 (Loughran *et al*, 2017), was used as a template to design the *Renilla* luciferase and the ZIKV
478 firefly luciferase reporters. The *Renilla* luciferase was amplified using the following
479 oligonucleotides 5´- TCCGCCCAGTTCCGCCCATTCTCCGC-3´ and 5´-

480 GCGCTCTAGATTATCTCGAGGTGTAGAAATAC- 3´ and then cloned back into the
481 pSGDLuc previously digested with *AvrII* and *XbaI* This will create a plasmid only expressing
482 the *Renilla* luciferase gene under the T7 or SV40 promoter.
483 The first 194 nucleotides of the ZIKV genome were cloned first in the pSGD plasmid using the
484 set of primers 5´-GCGCCTCGAGATAAGTTGTTGATCTGTGTGAATCAGAC-3´ and 5´-
485 GCGCAGATCTGCCCCCAAAGGGGCTCACACGGGCTAC-3´ in order to introduce this
486 fragment in frame with the 2A-firefly luciferase gene. Using this intermediate plasmid as a
487 template, the ZIKV-2A-firefly luciferase gene was later amplified with oligonucleotides 5´-
488 TCCGCCCAGTTCCGCCCATTCTCCGC-3´and 5´-
489 GATTCACACAGATCAACAACTccctatagtgagtc to introduce the T7 promoter upstream of the
490 ZIKV coding region; and 5´-GCTTTACTGGGGCTACGATCTTTTGC-3´ and 5´-
491 gactcactatagggAGTTGTTGATCTGTGTGAATC-3´ to amplify the ZIKV region. This was
492 cloned back into the pSGD plasmid previously digested with *AvrII* and *BglII* . This will create
493 a plasmid expressing the ZIKV-2A-firefly luciferase fused gene under the T7 or SV40
494 promoter.
495 **Luciferase assays**: Cells were transfected using Lipofectamine 3000 (Invitrogen)
496 with firefly and *Renilla* luciferase plasmids at the proportion of 98 ng and 2 ng respectively for
497 every $2x10^4$ cells in a 96-wells plate. For cell lysis and luminescence reaction, Dual-
498 Luciferase® Reporter Assay System (Promega) was used following the manufacturer's
499 instructions.
500
501 **Single-cell RNA sequencing analysis:** Processed, publicly available single-cell
502 RNA-seq data are available through the GEO accession number GSE110496 and
503 GSE116672. We downloaded processed single-cell data and metadata from the
504 supplementary information from the respective publication (Zanini *et al*, 2018a, 2018b).
505 Then, we used CellRouter (Lummertz da Rocha *et al*, 2018) to perform quality control,
506 normalization, analysis and visualize the expression of selected genes with log2 fold changes
507 > 0.15.
508
509
510 **AUTHOR CONTRIBUTIONS**
511 Conceptualization, T.R.J. and D.S.M.; Methodology, T.R.J. and D.S.M.; Formal Analysis and
512 Investigation, T.R.J.; *In silico* analysis, E.L.R., E.G.K., G.F.R.L.; Resources, D.S.M., B.F., N.I.
513 , Writing-Original Draft, T.R.J. and D.S.M., Writing-Review and editing, T.R.J., B.F., N.I. and
514 D.S.M., Visualization, T.R.J. and D.S.M., Supervision, D.S.M., Project Administration and
515 Funding Acquisition, D.S.M.

516 **DECLARATION OF INTERESTS**

517 The authors declare no competing interests.

518

519 **ACKNOWLEDGEMENTS**

520 This work was supported by Comissão de Aperfeiçoamento de Pessoal de Nível
521 Superior (CAPES) Computational Biology programme (23038.010048/2013-27), Conselho
522 Nacional de Desenvolvimento Científico e Tecnológico (CNPq) (1 311406/2017-3 and
523 407609/2018-0) and the Academy of Medical Sciences/U.K. (NAF004/1005) to D.S.M.,
524 Conselho Nacional de Desenvolvimento Científico e Tecnológico (CNPq) (41907/2017-7) to
525 T.R.J., BBSRC grant BB/S001336/1 and Wellcome Trust grant 201946/Z/16/Z to B.J.F; and
526 an Isaac Newton Trust Grant (18.40r), a Royal Society Research Grant (RGS\R1\191137) and
527 an Isaac Newton Trust/Wellcome Trust ISSF/University of Cambridge Joint Research Grant
528 to NI.

529

530 Multi-User Laboratory in Biological Studies (LAMEB) and LCME at UFSC.

531

532 **REFERENCES**

533 Ambrose RL & Mackenzie JM (2011) West Nile virus differentially modulates the unfolded
534 protein response to facilitate replication and immune evasion. *J Virol* 85: 2723–2732

535 Antunes KH, Fachi JL, de Paula R, da Silva EF, Pral LP, Dos Santos AÁ, Dias GBM, Vargas
536 JE, Puga R, Mayer FQ, *et al* (2019) Microbiota-derived acetate protects against
537 respiratory syncytial virus infection through a GPR43-type 1 interferon response. *Nat*
538 *Commun* 10: 3273

539 Axten JM, Romeril SP, Shu A, Ralph J, Medina JR, Feng Y, Li WHH, Grant SW, Heerding
540 DA, Minthorn E, *et al* (2013) Discovery of GSK2656157: An Optimized PERK Inhibitor
541 Selected for Preclinical Development. *ACS Med Chem Lett* 4: 964–968

542 Beltramello M, Williams KL, Simmons CP, Macagno A, Simonelli L, Quyen NTH, Sukupolvi-
543 Petty S, Navarro-Sanchez E, Young PR, de Silva AM, *et al* (2010) The human immune
544 response to Dengue virus is dominated by highly cross-reactive antibodies endowed
545 with neutralizing and enhancing activity. *Cell Host Microbe* 8: 271–283

546 Ben-Asouli Y, Banai Y, Pel-Or Y, Shir A & Kaempfer R (2002) Human interferon-gamma
547 mRNA autoregulates its translation through a pseudoknot that activates the interferon-
548 inducible protein kinase PKR. *Cell* 108: 221–232

549 Canino C, Luo Y, Marcato P, Blandino G, Pass HI & Cioce M (2015) A STAT3-
550 NFkB/DDIT3/CEBPβ axis modulates ALDH1A3 expression in chemoresistant cell
551 subpopulations. *Oncotarget* 6: 12637–12653

552 Chambers TJ, Hahn CS, Galler R & Rice CM (1990) Flavivirus genome organization,
553 expression, and replication. *Annu Rev Microbiol* 44: 649–688

554 Clavarino G, Cláudio N, Couderc T, Dalet A, Judith D, Camosseto V, Schmidt EK, Wenger
555 T, Lecuit M, Gatti E, *et al* (2012) Induction of GADD34 is necessary for dsRNA-
556 dependent interferon-β production and participates in the control of Chikungunya virus
557 infection. *PLoS Pathog* 8: e1002708

558 Czerkies M, Korwek Z, Prus W, Kochańczyk M, Jaruszewicz-Błońska J, Tudelska K, Błoński
559 S, Kimmel M, Brasier AR & Lipniacki T (2018) Cell fate in antiviral response arises in the
560 crosstalk of IRF, NF-κB and JAK/STAT pathways. *Nat Commun* 9: 493

561 Dalet A, Argüello RJ, Combes A, Spinelli L, Jaeger S, Fallet M, Vu Manh T-P, Mendes A,
562 Perego J, Reverendo M, *et al* (2017) Protein synthesis inhibition and GADD34 control
563 IFN-β heterogeneous expression in response to dsRNA. *EMBO J* 36: 761–782

564 Datan E, Roy SG, Germain G, Zali N, McLean JE, Golshan G, Harbajan S, Lockshin RA &
565 Zakeri Z (2016) Dengue-induced autophagy, virus replication and protection from cell
566 death require ER stress (PERK) pathway activation. *Cell Death Dis* 7: e2127

567 Deb A, Haque SJ, Mogensen T, Silverman RH & Williams BR (2001) RNA-dependent
568 protein kinase PKR is required for activation of NF-kappa B by IFN-gamma in a STAT1-
569 independent pathway. *J Immunol* 166: 6170–6180

570 Dickhout JG, Carlisle RE, Jerome DE, Mohammed-Ali Z, Jiang H, Yang G, Mani S, Garg SK,
571 Banerjee R, Kaufman RJ, *et al* (2012) Integrated stress response modulates cellular
572 redox state via induction of cystathionine γ-lyase: cross-talk between integrated stress
573 response and thiol metabolism. *J Biol Chem* 287: 7603–7614

574 Donnelly N, Gorman AM, Gupta S & Samali A (2013) The eIF2α kinases: their structures
575 and functions. *Cell Mol Life Sci* 70: 3493–3511

576 Donzé O, Deng J, Curran J, Sladek R, Picard D & Sonenberg N (2004) The protein kinase
577 PKR: a molecular clock that sequentially activates survival and death programs. *EMBO*
578 *J* 23: 564–571

579 Edgil D, Polacek C & Harris E (2006) Dengue virus utilizes a novel strategy for translation
580 initiation when cap-dependent translation is inhibited. *J Virol* 80: 2976–2986

581 Espada CE, da Rocha EL, dos Santos AA, Soares ZG, Malaquias G, Patrício DO, Kozlova
582 EG, dos Santos PF, Bordignon J, Sanford TJ, *et al* (2019) ISG15/USP18/STAT2 is a
583 molecular hub regulating autocrine IFN I-mediated control of Dengue and Zika virus
584 replication. *bioRxiv*

585 Espada-Murao LA & Morita K (2011) Delayed cytosolic exposure of Japanese encephalitis
586 virus double-stranded RNA impedes interferon activation and enhances viral
587 dissemination in porcine cells. *J Virol* 85: 6736–6749

588 Fernández-García L, Angulo J, Ramos H, Barrera A, Pino K, Vera-Otarola J & López-Lastra
589 M (2020) The internal ribosome entry site of the Dengue virus mRNA is active when
590 cap-dependent translation initiation is inhibited. *J Virol*

591 Fredericksen BL & Gale M Jr (2006) West Nile virus evades activation of interferon
592 regulatory factor 3 through RIG-I-dependent and -independent pathways without
593 antagonizing host defense signaling. *J Virol* 80: 2913–2923

594 Fusakio ME, Willy JA, Wang Y, Mirek ET, Al Baghdadi RJT, Adams CM, Anthony TG & Wek
595 RC (2016) Transcription factor ATF4 directs basal and stress-induced gene expression
596 in the unfolded protein response and cholesterol metabolism in the liver. *Mol Biol Cell*

597 27: 1536–1551

598 Gilfoy FD & Mason PW (2007) West Nile virus-induced interferon production is mediated by
599 the double-stranded RNA-dependent protein kinase PKR. *J Virol* 81: 11148–11158

600 Gillespie LK, Hoenen A, Morgan G & Mackenzie JM (2010) The endoplasmic reticulum
601 provides the membrane platform for biogenesis of the flavivirus replication complex. *J*
602 *Virol* 84: 10438–10447

603 Gjymishka A, Su N & Kilberg MS (2009) Transcriptional induction of the human asparagine
604 synthetase gene during the unfolded protein response does not require the ATF6 and
605 IRE1/XBP1 arms of the pathway. *Biochem J* 417: 695–703

606 Gladwyn-Ng I, Cordón-Barris L, Alfano C, Creppe C, Couderc T, Morelli G, Thelen N,
607 America M, Bessières B, Encha-Razavi F, *et al* (2018) Stress-induced unfolded protein
608 response contributes to Zika virus-associated microcephaly. *Nat Neurosci* 21: 63–71

609 Guimarães ES, Gomes MTR, Campos PC, Mansur DS, Dos Santos AA, Harms J, Splitter G,
610 Smith JA, Barber GN & Oliveira SC (2019) Cyclic Dinucleotides Trigger STING-
611 Dependent Unfolded Protein Response That Favors Bacterial Replication. *J Immunol*
612 202: 2671–2681

613 Gullberg RC, Steel JJ, Pujari V, Rovnak J, Crick DC & Perera R (2018) Stearoly-CoA
614 desaturase 1 differentiates early and advanced dengue virus infections and determines
615 virus particle infectivity. *PLoS Pathog* 14: e1007261

616 Harding HP, Novoa I, Zhang Y, Zeng H, Wek R, Schapira M & Ron D (2000) Regulated
617 translation initiation controls stress-induced gene expression in mammalian cells. *Mol*
618 *Cell* 6: 1099–1108

619 Hou J-N, Chen T-H, Chiang Y-H, Peng J-Y, Yang T-H, Cheng C-C, Sofiyatun E, Chiu C-H,
620 Chiang-Ni C & Chen W-J (2017) PERK Signal-Modulated Protein Translation Promotes
621 the Survivability of Dengue 2 Virus-Infected Mosquito Cells and Extends Viral
622 Replication. *Viruses* 9

623 Huang Y, Chuang AY, Romano R-A, Liégeois NJ, Sinha S, Trink B, Ratovitski E & Sidransky
624 D (2010) Phospho-DeltaNp63alpha/NF-Y protein complex transcriptionally regulates
625 DDIT3 expression in squamous cell carcinoma cells upon cisplatin exposure. *Cell Cycle*
626 9: 328–338

627 Jackson RJ, Hellen CUT & Pestova TV (2010) The mechanism of eukaryotic translation
628 initiation and principles of its regulation. *Nat Rev Mol Cell Biol* 11: 113–127

629 Kaempfer R, Ilan L, Cohen-Chalamish S, Turgeman O, Namer LS & Osman F (2019)
630 Control of mRNA Splicing by Intragenic RNA Activators of Stress Signaling: Potential
631 Implications for Human Disease. *Front Genet* 10: 464

632 Kårehed K, Dimberg A, Dahl S, Nilsson K & Oberg F (2007) IFN-gamma-induced
633 upregulation of Fcgamma-receptor-I during activation of monocytic cells requires the
634 PKR and NFkappaB pathways. *Mol Immunol* 44: 615–624

635 Krishnamoorthy T, Pavitt GD & Zhang F (2001) Tight binding of the phosphorylated α
636 subunit of initiation factor 2 (eIF2α) to the regulatory subunits of guanine nucleotide
637 exchange factor eIF2B is required for …. *and cellular biology*

638 Lee Y-Y, Cevallos RC & Jan E (2009) An upstream open reading frame regulates translation

639 of GADD34 during cellular stresses that induce eIF2alpha phosphorylation. *J Biol Chem*
640 284: 6661–6673

641 Loughran G, Howard MT, Firth AE & Atkins JF (2017) Avoidance of reporter assay
642 distortions from fused dual reporters. *RNA* 23: 1285–1289

643 Lummertz da Rocha E, Rowe RG, Lundin V, Malleshaiah M, Jha DK, Rambo CR, Li H, North
644 TE, Collins JJ & Daley GQ (2018) Reconstruction of complex single-cell trajectories
645 using CellRouter. *Nat Commun* 9: 892

646 Ma Y & Hendershot LM (2004) Herp is dually regulated by both the endoplasmic reticulum
647 stress-specific branch of the unfolded protein response and a branch that is shared with
648 other cellular stress pathways. *J Biol Chem* 279: 13792–13799

649 Novoa I, Zeng H, Harding HP & Ron D (2001) Feedback Inhibition of the Unfolded Protein
650 Response by GADD34-Mediated Dephosphorylation of eIF2α. *J Cell Biol* 153: 1011–
651 1022

652 Ohoka N, Yoshii S, Hattori T, Onozaki K & Hayashi H (2005) TRB3, a novel ER stress-
653 inducible gene, is induced via ATF4-CHOP pathway and is involved in cell death. *EMBO*
654 *J* 24: 1243–1255

655 Overby AK, Popov VL, Niedrig M & Weber F (2010) Tick-borne encephalitis virus delays
656 interferon induction and hides its double-stranded RNA in intracellular membrane
657 vesicles. *J Virol* 84: 8470–8483

658 Pakos-Zebrucka K, Koryga I, Mnich K, Ljujic M, Samali A & Gorman AM (2016) The
659 integrated stress response. *EMBO Rep* 17: 1374–1395

660 Pause A, Belsham GJ, Gingras AC, Donzé O, Lin TA, Lawrence JC Jr & Sonenberg N
661 (1994) Insulin-dependent stimulation of protein synthesis by phosphorylation of a
662 regulator of 5'-cap function. *Nature* 371: 762–767

663 Peña J & Harris E (2011) Dengue virus modulates the unfolded protein response in a time-
664 dependent manner. *J Biol Chem* 286: 14226–14236

665 Pestova TV, de Breyne S, Pisarev AV, Abaeva IS & Hellen CUT (2008) eIF2-dependent and
666 eIF2-independent modes of initiation on the CSFV IRES: a common role of domain II.
667 *EMBO J* 27: 1060–1072

668 Poulin F, Gingras AC, Olsen H, Chevalier S & Sonenberg N (1998) 4E-BP3, a new member
669 of the eukaryotic initiation factor 4E-binding protein family. *J Biol Chem* 273: 14002–
670 14007

671 Ran FA, Hsu PD, Wright J, Agarwala V, Scott DA & Zhang F (2013) Genome engineering
672 using the CRISPR-Cas9 system. *Nat Protoc* 8: 2281–2308

673 Rivas-Estilla AM, Svitkin Y, Lopez Lastra M, Hatzoglou M, Sherker A & Koromilas AE (2002)
674 PKR-dependent mechanisms of gene expression from a subgenomic hepatitis C virus
675 clone. *J Virol* 76: 10637–10653

676 Robert F, Kapp LD, Khan SN, Acker MG, Kolitz S, Kazemi S, Kaufman RJ, Merrick WC,
677 Koromilas AE, Lorsch JR, *et al* (2006) Initiation of protein synthesis by hepatitis C virus
678 is refractory to reduced eIF2.GTP.Met-tRNA(i)(Met) ternary complex availability. *Mol*
679 *Biol Cell* 17: 4632–4644

680 Roth H, Magg V, Uch F, Mutz P, Klein P, Haneke K, Lohmann V, Bartenschlager R, Fackler

681 OT, Locker N, *et al* (2017) Flavivirus Infection Uncouples Translation Suppression from
682 Cellular Stress Responses. *MBio* 8

683 Schmidt EK, Clavarino G, Ceppi M & Pierre P (2009) SUnSET, a nonradioactive method to
684 monitor protein synthesis. *Nat Methods* 6: 275–277

685 Sharma M, Bhattacharyya S, Sharma KB, Chauhan S, Asthana S, Abdin MZ, Vrati S & Kalia
686 M (2017) Japanese encephalitis virus activates autophagy through XBP1 and ATF6 ER
687 stress sensors in neuronal cells. *J Gen Virol* 98: 1027–1039

688 Song Y, Mugavero J, Stauft CB & Wimmer E (2019) Dengue and Zika Virus 5' Untranslated
689 Regions Harbor Internal Ribosomal Entry Site Functions. *MBio* 10

690 Tan Z, Zhang W, Sun J, Fu Z, Ke X, Zheng C, Zhang Y, Li P, Liu Y, Hu Q, *et al* (2018) ZIKV
691 infection activates the IRE1-XBP1 and ATF6 pathways of unfolded protein response in
692 neural cells. *J Neuroinflammation* 15: 275

693 Umareddy I, Pluquet O, Wang QY, Vasudevan SG, Chevet E & Gu F (2007) Dengue virus
694 serotype infection specifies the activation of the unfolded protein response. *Virol J* 4: 91

695 Wang K, Zou C, Wang X, Huang C, Feng T, Pan W, Wu Q, Wang P & Dai J (2018)
696 Interferon-stimulated TRIM69 interrupts dengue virus replication by ubiquitinating viral
697 nonstructural protein 3. *PLoS Pathog* 14: e1007287

698 Wang Q, Xin X, Wang T, Wan J, Ou Y, Yang Z, Yu Q, Zhu L, Guo Y, Wu Y, *et al* (2019)
699 Japanese Encephalitis Virus Induces Apoptosis and Encephalitis by Activating the
700 PERK Pathway. *J Virol* 93

701 Wek RC, Jiang H-Y & Anthony TG (2006) Coping with stress: eIF2 kinases and translational
702 control. *Biochem Soc Trans* 34: 7–11

703 Whelan JN, Li Y, Silverman RH & Weiss SR (2019) Zika Virus Production Is Resistant to
704 RNase L Antiviral Activity. *J Virol* 93

705 Young SK & Wek RC (2016) Upstream Open Reading Frames Differentially Regulate Gene-
706 specific Translation in the Integrated Stress Response. *J Biol Chem* 291: 16927–16935

707 Young SK, Willy JA, Wu C, Sachs MS & Wek RC (2015) Ribosome Reinitiation Directs
708 Gene-specific Translation and Regulates the Integrated Stress Response. *J Biol Chem*
709 290: 28257–28271

710 Zamanian-Daryoush M, Mogensen TH, DiDonato JA & Williams BR (2000) NF-kappaB
711 activation by double-stranded-RNA-activated protein kinase (PKR) is mediated through
712 NF-kappaB-inducing kinase and IkappaB kinase. *Mol Cell Biol* 20: 1278–1290

713 Zanini F, Pu S-Y, Bekerman E, Einav S & Quake SR (2018a) Single-cell transcriptional
714 dynamics of flavivirus infection. *Elife* 7

715 Zanini F, Robinson ML, Croote D, Sahoo MK, Sanz AM, Ortiz-Lasso E, Albornoz LL, Rosso
716 F, Montoya JG, Goo L, *et al* (2018b) Virus-inclusive single-cell RNA sequencing reveals
717 the molecular signature of progression to severe dengue. *Proc Natl Acad Sci U S A* 115:
718 E12363–E12369

719 Zhang J, Lan Y, Li MY, Lamers MM, Fusade-Boyer M, Klemm E, Thiele C, Ashour J &
720 Sanyal S (2018) Flaviviruses Exploit the Lipid Droplet Protein AUP1 to Trigger
721 Lipophagy and Drive Virus Production. *Cell Host Microbe* 23: 819–831.e5